Low inductance winding installed around GIS core-conductor damps Very Fast Transient Overvoltages

R. Malewski, J. H. Park, W. H. Heo

Abstract **- A low-inductance winding wound around GIS center-conductor (core) can contribute to damping of Very Fast Transient Overvoltage (VFTO) generated by operation of disconnect-switch (DS) in Gas Insulated Station. High-frequency spectral-components of VFTO induce magnetic field around the GIS core. This field induces a current in a low-inductance winding wound around the core. Energy dissipated in the winding resistance contributes to VFTO damping. As opposed to other VFTO systems there is no magnetic core saturation and no need for auxiliary contacts of the DS with series resistor.**

Concept and background of the proposed VFTO damping system are presented here and experimental results will be reported in subsequent papers.

Keywords: **VFTO damping, high-frequency magnetic-field, low-inductance winding, loss in the winding resistance**

I. INTRODUCTION

High Voltage Gas Insulated switchgear generates VFTO with magnitude exceeding 2 p.u, and frequency spectrum extended beyond 100 MHz [1]-[3]. Several methods have been considered to attenuate such overvoltages: ferrite or nanocrystalline rings installed around the GIS core [4]-[6], cavity resonator tuned to the dominant frequency of VFTO-spectrum [7], DS with a resistor in series to auxiliary contacts or breaker with the slow contact-movement [8]-[11]. These concepts are sound and have been tried by the utilities operating Ultra High Voltage transmission, but their implementation is hampered by technical drawbacks such as saturation of ferrite and nanocrystalline rings, very high cost of DS with auxiliary contacts, and absorption of VFTO energy at only a narrow band of its broad frequency-spectrum.

Another concept of VFTO mitigation consists in installation of a resistive coating around GIS core conductor, which dissipates energy of VFTO higher spectral-components, pushed to this outer layer by skin effect. This concept of resistive coating has been examined but it turns out impractical, since the required length is excessively long. At present no coating material with the required resistivity is available to implement this solution in practice. However, the required resistance can be attained by winding a low-inductance coil of a resistive wire installed around and connected to GIS core [12].

Ryszard Malewski is consultant with Malewski Electric Inc. in Montreal, QC. Canada. (e-mail malewski@ieee.org).

June Hee Park and Woo Hung Heo are with Hyosung Corporation, Chang-won, Korea (e-mail junehee@hyosung.com and hwh@hyosung.com).

Paper submitted to the International Conference on Power System Transients(IPST2017)in Seoul, Republic of Korea June 26-29, 2017.

A familiar example of practical use of skin-effect in electric conductors[13]-[14] has been the silver plated copper wire, which at low frequency conducts a major part of the current through the thick copper core, but the high frequency current flows in the relatively thin silver-layer.

The presented concept works a *au rebours*. A low-inductance coil installed around the GIS core conductor and connected to it at the winding terminals does not affect the flow of power-frequency heavy-current. However, the superposed very-fast transient-current is forced to flow in the low inductance winding and to dissipate energy in the winding resistance.

An obvious advantage of such device is lack of saturation by heavy current at power frequency, and dissipation of the transient overvoltage energy in the winding resistance that results in attenuation of the overvoltage magnitude.

This report presents an investigation of Ayrton-Perry style winding made of enameled wire used to damp VFTO. Such winding meets the requirement of sufficient resistance to damp VFTO and has high enough dielectric strength to withstand the stress [15]-[16] .

A computer model of GIS section equipped with the low-inductance winding was developed to simulate the low-inductance winding by Equivalent Resistance Coating (ERC). This model demonstrated an effective attenuation of high-frequency components of VFTO superimposed on power-frequency current.

Practical implementation of the proposed method is considered by the manufacturer of HV transformers and shunt reactors designed for connection to GIS and switching by SF6 breakers and disconnect switches.

Results of measurements taken on an experimental stand will be reported in the next paper.

II. ELECTRIC FIELD ALONG TANGENTIAL SURFACES OF GIS CORE, INSULATING SUPPORT, ERC AND OUTER CONDUCTOR

The GIS core is made of thick-wall aluminum tube. Equivalent Resistive Coating referred to as (ERC) constitutes a low-inductance winding composed of two parallel wires wound in opposite direction on an insulating support.

In the computer model this Ayrton-Perry style winding is simulated by a thin-wall tube made of resistive material and connected at its both ends to the core. ERC and the core form parallel conductors and the GIS current is split between them. At power frequency nearly all current flows in the core and none in ERC, since its resistance is much higher that that of the core.

However, in frequency range of MHz the skin effect forces GIS current to flow in ERC and to dissipate energy in ERC resistance. The current division between core and ERC is determined by the requirement that the electric field (E) along the surface of adjacent, parallel connected conductors must be the same. The electric field $E_{core}=J_{core}\cdot\rho_{core}$, where: J_{core} is current density at the core **outer** surface and ρ_{core} is the core material resistivity.

The electric field at ERC **inner** surface $E_{ERC}=J_{ERC}\cdot\rho_{ERC}$ is determined by current density at the surface of ERC and its resistivity. When ERC is directly laid on core the condition $E_{core}=E_{ERC}$ must be fulfilled.

However, an insulating support of the winding is inserted between core and ERC, as shown in Fig 1a. This forms a closed loop between the core and ERC. The area S enclosed by this loop depends on thickness of the insulating support and the distance ℓ between ERC ends connected to the core. Magnetic flux Φ flowing through the area S induces a voltage U in this loop that increases with frequency of the current flowing in core. An electric field at ERC inner surface becomes then the sum of $E_{ERC}=E_{core}+E_{induced}$; where: the $E_{induced}=U/\ell$, as shown schematically in Fig1 b.

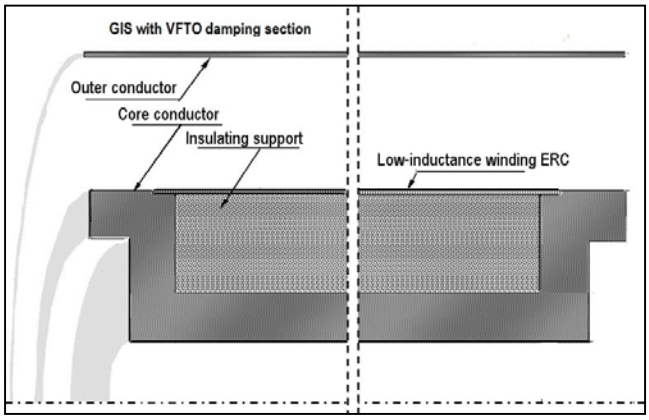

Fig.1a. Sketch of GIS section along its axis, with ERC connected in parallel to the core and insulating support inserted between the core and ERC to damp VFTO.

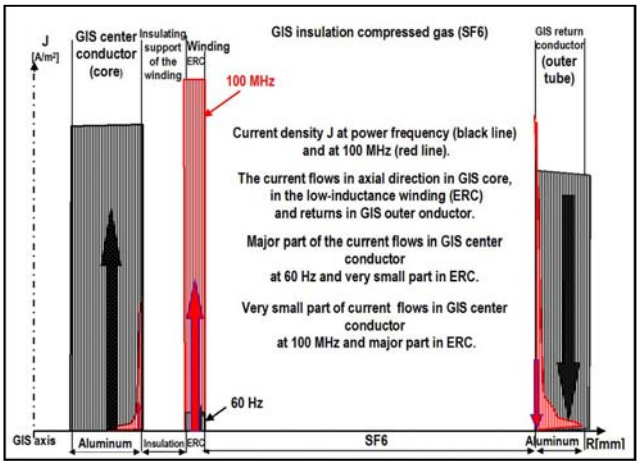

Fig.1b. Current density J distribution in the GIS section at power frequency (black line) and at 100 MHz (red line) that corresponds to high-frequency spectral-component of VFTO.

The high-frequency magnetic flux Φ in the insulating support induces voltage U that controls the current in the low-inductance winding ERC.

III. Current Density And Magnetic Field Distribution

A. Computer model.

The current in ERC $I_{ERC}(f)$ is derived from the current density J and magnetic field H distribution calculated as a function of frequency f on the computer model. The current flowing in the core was set as $I_{core\text{-}total}=4A$, and the distance between ERC ends was set at $\ell=1$ m, to standardize the format of computer simulation output. Dimensions of the GIS components and material resistivity are shown on following pages, but the calculation formulae are given below.

Owing to axial symmetry the model simulates a segment of one quarter of the GIS, and the core segment current is set at $I_{core}=¼\ I_{core\text{-}total}=1A$.

Magnetic field H between the core and ERC is the function of radius R. At the core outer surface:

$$H_{ERC}=\frac{I_{core-total}}{2\pi R_{ERC}}=16A/m$$

and at ERC inner surface:

$$H_{core}=\frac{I_{core-total}}{2\pi R_{core}}=32A/m$$

where $R_{core}=20\cdot10^{-3}$m and $R_{ERC}=39\cdot10^{-3}$m.

Magnetic flux Φ in the loop formed by the insulating support cross section is given by:

$$\Phi=\mu\cdot\int_{20}^{39}H(R)\cdot dR=\frac{I_{core-total}\cdot\mu}{2\pi}\cdot\ln\left(\frac{39}{20}\right)=5.43\cdot10^{-7}Vs$$

where R is within: $20\cdot10^{-3}\le R\le39\cdot10^{-3}$m, and $\mu=4\pi\cdot10^{-7}$H/m.

The electric field induced by this flux equals:

$E_{induced}=2\cdot\pi\cdot f\cdot\Phi=3.36V/m$, at $f=10^6$Hz;

and $E_{ERC}\approx E_{induced}$ since $E_{core}<<E_{ERC}$.

Current density at ERC surface, with $\rho_{ERC}=62\cdot10^{-6}\Omega m$

$J_{ERC}=E_{ERC}/\rho_{ERC}=3.36/62\cdot10^{-6}=5.419\cdot10^4A/m^2$.

Current in the ¼ segment of ERC $I_{ERC}=J_{ERC}\cdot A_{ERC}=$

$=¼\cdot5.419\cdot10^4\cdot248\cdot10^{-6}=3.36A$,

where $A_{ERC}=\pi\cdot(40^2-39^2)\cdot10^{-6}=248\cdot10^{-6}m^2$.

For a fixed geometry and ERC material resistivity ρ_{ERC} the current forced to flow in ERC depends only on frequency.

It follows that effectiveness of damping high-frequency spectral components in VFTO increases exponentially with their frequency.

At 1MHz the current in $I_{ERC}=3.36\cdot I_{core}$.

At 10 MHz the current in $I_{ERC}=33.6\cdot I_{core}$

At 100MHz the current in $I_{ERC}=336\cdot I_{core}$

However at 100 Hz the current in $I_{ERC}=0.000336\cdot I_{core}$.

B. Input data to the VFTO damping system model

GIS section ℓ=1m long, is composed of coaxial components: **Core** center conductor, **ERC** Equivalent Resistive Coating and **Out**er return conductor.

DC resistance of the GIS ℓ=1m section of ¼GIS segment used in the model. Core and Out resistivity $\rho_{alu}=3\cdot10^{-8}\Omega m$

TABLE 1
DIMENSIONS AND DC RESISTANCE OF THE COMPONENTS

	Inner radius	Outer radius	Cross section	DC resistance
Units	mm	mm	m^2	**Ω**
Core	10	20	$0.942\cdot10^{-3}$	$12.7\cdot10^{-5}$
ERC	39	40	$0.248\cdot10^{-3}$	1.00
Out	88	90	$1.118.10^{-3}$	10.7·10-5

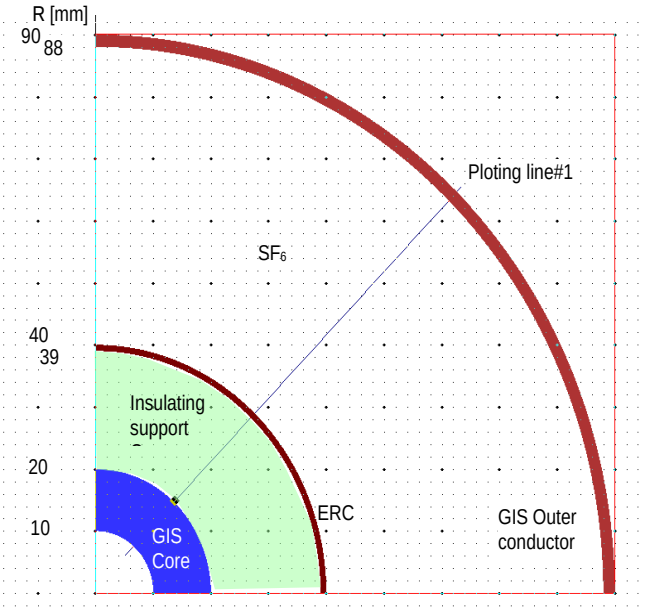

Fig.2. FEM Model. Segment of ¼ GIS cross section. Plotting line #1.

Simulation of magnetic field and current density at 1 MHz with the current imposed in: core 1A, in ERC 3.36A and in Out 4.36 A.

Simulation yielded resistance and inductance of ¼GIS segment shown below:

Impedance Matrix at 1 MHz (Distributed (Ohm/m, H/m)

	Core	ERC40
Core	(0.013749, 1.1836E-006)	(0.0037068, 6.3959E-007)
ERC40	(0.0037068, 6.3959E-007)	(1.0108, 6.3621E-007)

Fig.3. Resistance and inductance of core and ECR segment at 1 MHz.

ERC resistance 1.0108 Ω did not change from DC to 1 MHz, but core resistance $13.7\cdot10^{-3}$ Ω increased 100 times.

This increase of core resistance is expected, since skin effect forces current to flow in the narrow layer at the core outer surface.

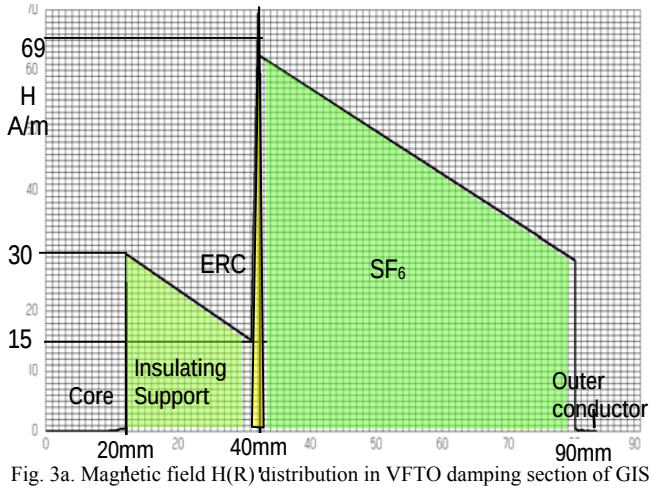

Fig. 3a. Magnetic field H(R) distribution in VFTO damping section of GIS at 1 MHz. I_{core}=1A; I_{ERC}=3.36A: $\mathbf{E_{induced}=3.36V/m}$; $\mathbf{E_{ERC}= 3.36V/m}$

Fig. 3b. Current density J(R) distribution in VFTO damping section of GIS at 1 MHz. Values read from the graph confirm analog calculations:

J_{ERC}=54000A/m². $\mathbf{I_{ERC}}$=¼ J_{ERC}· A_{ERC}=¼ 54 10^3 0.248 10^{-3}=**3.347A**

IV. ERC LOW-INDUCTANCE (AYRTON-PERRY) WINDING CALCULATION FOR THE GIS MODEL

A. Magnetic field pattern around the winding

Ayrton-Perry winding is composed of two equal-length sections of the enameled wire wound clockwise and anti-clockwise as single layer on an insulating support. These two wires are connected in parallel

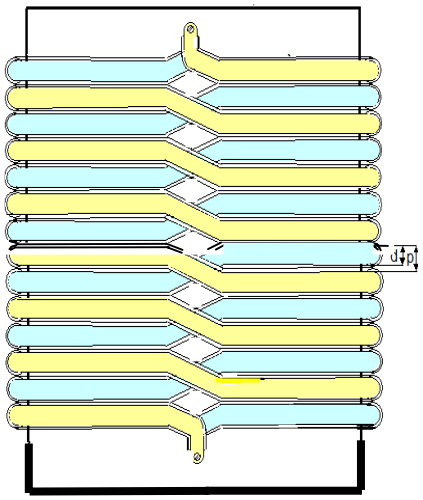

Fig.4. Ayrton-Perry winding: 1.15<p<1.20 (pitch), d- wire diameter. Time constant $T=L/R=(\mu\cdot d^2/8\cdot\rho)\ [\ln(4\cdot p/\pi\cdot d)+¼]$.

Magnetic field pattern of Ayrton-Perry winding corresponds to that of a thin-wall tube that carries current in axial direction only. The axial component of the magnetic field is cancelled by the current circulating in clockwise and anticlockwise wound turns.
The azimuthal (hoop) field component of the two windings add up, and its magnitude is determined by the sum of two currents circulating in the windings wound in opposite direction [12]. To reduce the winding stray inductance the pitch has to be minimized and crossing of the opposite direction wound wires has to be located on a vertical line on both sides of the insulating support. The winding process is facilitated by flattening the support cylindrical profile on opposite sides.

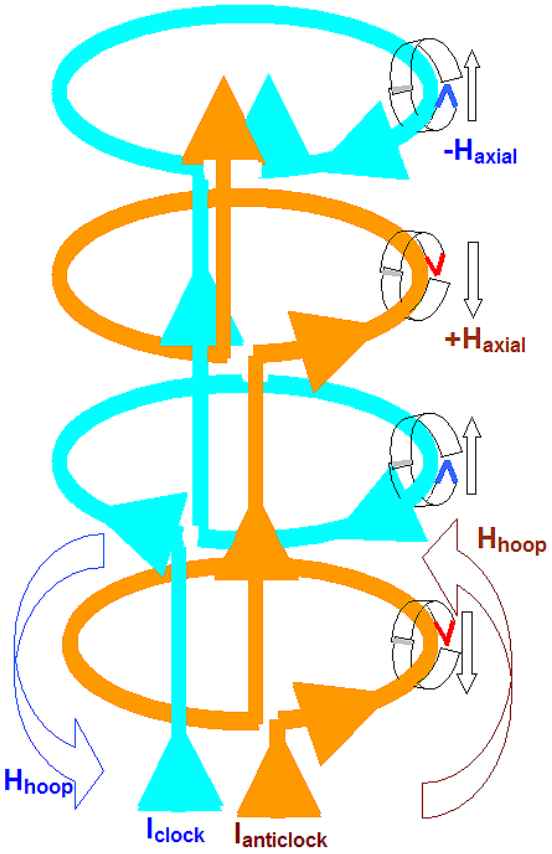

Fig.5. Compensation of axial magnetic field in Ayrton-Perry winding.

Winding parameters are dictated by the energy dissipated in the winding $E_{A\text{-}P}=\int R\, I(t)^2=\int U(t)^2/R$ by an impulse of a given duration and on the winding dielectric withstand.
The wire volume determines the adiabatic temperature-rise of the winding, and the winding voltage drop is determined by its dielectric strength. The choice of winding resistance is a trade off these two factors.

A high-resistivity alloy, such as NiCr (80%-20%) with the epoxy resin coated winding is used for High Voltage impulse measuring dividers and impulse current measuring shunts.

B. Dielectric strength of Ayrton-Perry winding

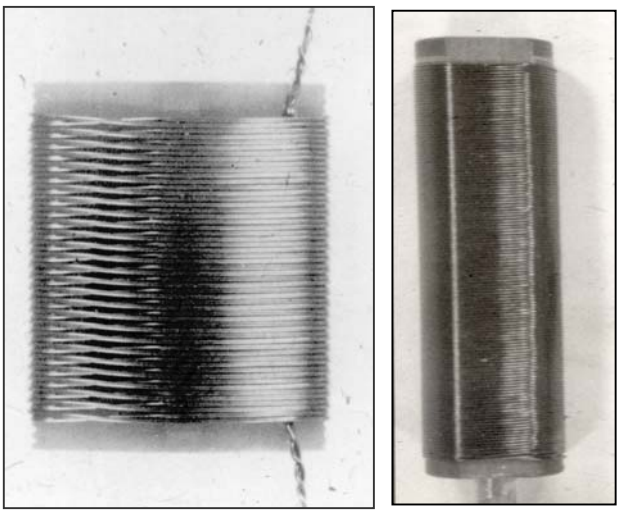

Fig. 6. Picture of Ayrton-Perry winding used in impulse current measuring shunts and voltage dividers.

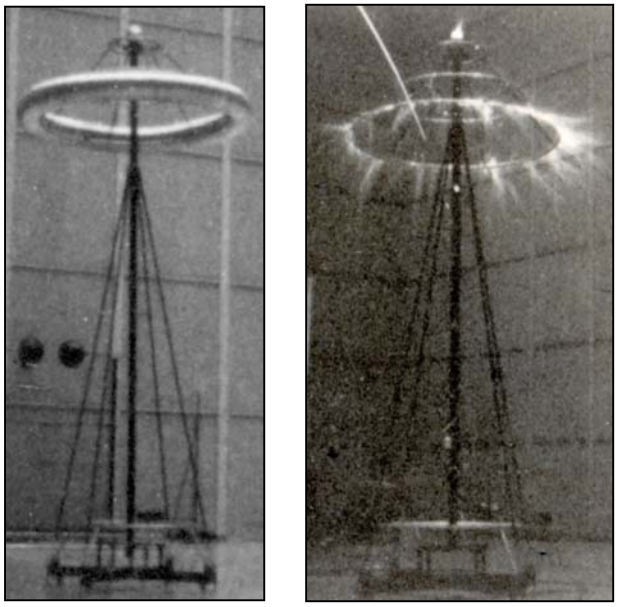

Fig,.7. Two pictures of 2.5 MV impulse voltage-divider made of enameled NiCr wire wound on insulating tube according to Ayrton-Perry style and covered by thin epoxy coating [16].

The left picture shows the divider with a large diameter toroid electrode that controls uniform field distribution along the winding stressed by 2.5 MV impulse. The right picture shows the same divider but with a thin ring.

The divider ring electrode cannot withstand the rated 2.5 MV impulse without intense corona discharges, but the winding is free from discharges 15] [16].

The coating of epoxy resin increases dielectric strength of Ayrton-Perry winding, and once applied to GIS core the winding strength increases further in SF_6. This confirms applicability of such winding to VFTO damping.

B. Example of Ayrton-Perry winding

The model is designed to demonstrate damping of VFTO in GIS. ERC resistance equal to Ayrton-Perry winding resistance was selected to ensure the effective damping of the high-frequency components of VFTO and to facilitate preparation of the model using available materials.

Enameled copper wire was chosen for convenience of making first Ayrton-Perry winding that involved lathe-operator training and inevitable trial-winding sent to scrap.

The winding is composed of two sections of 300 turns each, wound clockwise and anti-clockwise on the winding insulating support with outer radius r=39 mm. The winding physical length was set at ℓ=1 m. The wire length of each winding attains L_w=75 m.

The complete winding resistance was set at R_{DC} =0.25 Ω.

Enameled copper wire AWG 13 is wound with a very small pitch, and the insulating support tube, with wire crossing aligned in vertical line. AWG 13 wire diameter equals to d=1.83 10^{-3} m, cross section area S=2.63 10^{-6} m^2. The time constant T=16 ns for tightly wound winding.

DC resistance of 1m section of wire R_{AWG13}=6.55 10^{-3} Ω, assuming resistivity of ρ_{Cu}=1.724 10^{-8} Ωm. Resistance DC of Ayrton-Perry winding composed of two parallel 300 turn sections amounts to 2.46 Ω, close enough to the required 2.5 Ω.

Fig.8. Laboratory test set-up with ferrite rings and Ayrton-Perry winding for preliminary low-voltage comparison of VFTO damping effectiveness.

At this stage no experimental results are available to assess the performance of conventional ferrite rings versus the proposed low-inductance winding. The investigation will continue using a real-scale GIS model with HV gas insulated switch, and HV source.

V. Further Work

The experimental stand design and development involves advanced measuring devices and technique to record simultaneously waveform of transient overvoltage at two or more locations. High-Voltage .capacitive dividers built in the GIS manhole covers have to cover very broad frequency range from a few Hertz to more than 100 MHz, with dynamic range high enough to record transient overvoltage up to 3 p.u. and also 1 p.u. power frequency voltage. Pioneering work in this field has been done by Chinese research scientists [17] [18], published and generously shared with our research community.

VI. Discussion

The concept of damping VFTO by directing the high-frequency current to a parallel path where the energy of VFTO high-frequency spectral-components is dissipated, can be applied to the high-voltage transformers and shunt reactors switched by gas-insulated DS.

The lead connecting transformer-bushing lower-terminal to the high-voltage winding is usually installed in a copper tube connected to the lead at one point. The copper tube acts as a shield to reduce the electric field distribution around the lead, which is made of a stranded, flexible copper conductor to carry the heavy load current [19].

It is feasible to replace the copper tube by Ayrton-Perry winding wound on sections of insulating tube and connected to the lead at both terminals of the winding. Properly chosen resistance of such winding will dissipate energy of VFTO high-frequency spectral components and contribute to their damping.

VII. Conclusions

Another method is presented to attenuate Very-Fast Transient Overvoltage (VFTO) generated by gas insulated breakers and switches in Gas Insulated Stations (GIS). This method consists in winding enameled wire on an insulating support around center conductor of the GIS section located near the breaker or switch. The wire is wound according to Ayrton-Perry style to attain very low inductance, and is connected at both ends to GIS core conductor

Such winding behaves as resistive coating layer and dissipates energy carried by VFTO traveling from the switch to GIS. At power frequency there is practically no current in this low-inductance winding and the load current flows in aluminum center-conductor. However VFTO high-frequency current is forced by skin effect to flow in this winding and to dissipate energy of high-frequency components in the winding resistance.

Ayrton-Perry resistive-wire winding coated with epoxy can withstand high dielectric stress. It has been applied to High-Voltage impulse measuring dividers and impulse current measuring shunts. Such epoxy covered winding can withstand more than 500 kV per one meter of winding length in the lightning-impulse voltage divider exposed to ambient air, and certainly to a higher stress in SF_6 gas.

VFTO are particularly dangerous to internal insulation of bushings, transformers, reactors and apparatus directly connected to GIS at the Ultra High-Voltage systems. Ayrton-Perry resistive winding can effectively protect this expensive and strategically important equipment. The proposed VFTO damping system is not affected by saturation of magnetic cores, absorption of only one spectral frequency of VFTO spectrum and may substitute for expensive additional contacts with series-resistor in gas-insulated breakers and disconnect switches. These factors are considered as limitations of other devices presently used to suppress these overvoltages.

VII. Acknowledgements

Comments and advice provided by Professor Weidong Liu form Tsinghua University are acknowledged here and very much appreciated.

We are obliged to the Management of Hyosung Corporation for their interest in the project and support in development of the HV test stand.

VIII. References

1. Y. Shu, W. Chen, Z. Li, M. Dai, C. Li, W. Liu, X. Yan, "Experimental Research on VFTO in 1100-kV in Gas-Insulated Switchgear", *IEEE Trans.,* Vol. PWRD-28, Nr. 1, 2012, p.458-466.
2. CIGRE Working Group AG.D1, "Very Fast Transient Overvoltage in Gas Insulated Stations", *CIGRE Brochure 519*, Paris 2012.
3. R. Mohana, M. Joy, M. Thomas, B. P., Singh, ”Frequency Characteristics of Very Fast Transient Currents in a 245-kV GIS”, *IEEE Trans*. Vol. PWRD-20, Nr.4, 2005, pp. 2450-2457.
4. M. Szewczyk, K. Kutorasiński, J. Pawłowski, W. Piasecki, M. Florkowski, "Advanced Modeling of Magnetic Cores for Damping of High-Frequency Power System Transients", *IEEE Trans*. Vol PWRD-31, Nr. 5, 2016, p2431-2439.
5. J. He, Y. Guan, W. Chen, W. Liu, X. Li. Dai, Y. Cai, "Experimental Research and Simulation on VFTO Mitigation by Ferrite Rings in UHV GIS", *IEEE Trans*. Vol. PWRD-30, Nr. 2, 2015, p.940-948.
6. U. Riechert, et all. "Mitigation of very Fast Transient Overvoltages in Gas Insulated UHV Substations", *CIGRE* A3_110, Paris 2012.
7. J. Smajic, A. Shoory, S. Burow, W. Holaus, U. Riechert, "Simulation-based Design of HF Resonators for Damping Very Fast Transients in GIS" *IEEE Trans*. Vol. PWRD-29, Nr. 6, 2014, p.2528-2533.
8. Szewczyk, M., Piasecki, W., Wroński, M., Kutorasiński, K., "New Concept for VFTO Attenuation in GIS with Modified Disconnector Contact System", *IEEE Trans*. Vol PWRD-30, Nr. 5, 2015, p2138-2145.
9. Y. Yamagata, K. Tanaka, S. Nishiwaki, "Suppression of VFTO in 1000 kV GIS by Adopting Resistor-Fitted Disconnector", *IEEE Trans*. Vol. PWRD-11, Nr. 2, 1996, p.872-880.
10. W.J. Chen, H. Wang, B. Han, L. Wang, G.M. Ma, G.C. Yue, Z.B. Li, H. Hu, "Study on the Influence of Disconnector Characteristics on VFTO in 1100kV Gas Insulated Switchgears", *IEEE Trans.* Vol. PWRD-30, Nr. 4, 2015, p.2037-2044.
11. H. Tanae, E. Matsuzaka, I. Nishida, I. Mataori,M. Tsukushi, K. Hirasawa, „High-Frequency Reignition Current and Its Influence on Electrical Durability of Circuit Breakers Associated with Shunt-Reactor Current Switching”, *IEEE Trans*. Vol. PWRD-19, Nr. 3, 2004, pp. 1105-1111..
12. R.L. Davis, "Design Formulae for Non-Reactive High-Voltage Pulse Resistors", *IEEE Trans*. Vol. PMP-1, Nr. 2, 1965, p 3-23
13. R. Malewski, C.T. Nguyen, K. Feser, N. Hyltén-Cavallius, "Elimination of the skin effect error in heavy current shunts", *IEEE Trans*. Vol. PAS-100, Nr.3, 1981, p.1333-1340.
14. R. Malewski, "Measurements of Transient Skin Effect Within Nonlinear Conductors", *IEEE Trans*. Vol. PAS-91, No. 5, 1972, pp. 1881-1886.
15. R. Malewski, "Wirewound Shunts for Measurement of Fast Current Impulses", *IEEE Trans.* Vol. PAS-103, No. 10, 1984, pp. 2927-2933
16. R. Malewski, S.P. Maruvada, "Computer Assisted Design of Impulse Voltage Dividers", *IEEE Trans*. Vol. PAS-95, No. 4, 1976, pp. 1267-1274.
17. Y. Gonghang, L. Weidong, C. Weijiang, G. Yongang, L. Zhibing, "Development of Full Bandwidth Measurement of VFTO in UHV GIS", ", *IEEE Trans.* Vol. PWRD-28, Nr. 4, 2013, p.2250-2558.
18. G,M. Ma, C.R. Li, W.J. Chen, M. Chen, Z.L. Sun, W.D. Ding, Z.B. Li, "Very Fast Transient Overvoltage Measurement with Dielectric Window", *IEEE Trans*. Vol. PWRD-29, Nr. 5, 2014, p.2410-2416.
19. CIGRE Working Group A2/C4.39, "Electrical Transients Interaction between Transformers and Power System".*CIGRE Brochure*, Paris 2013.